Acta Cryst E
CRYSTALLOGRAPHIC COMMUNICATIONS
ISSN 2056-9890

Quantitative analysis of weak non-covalent interactions in (*Z*)-3-(4-chlorophenyl)-2-phenylacrylonitrile: insights from *PIXEL* and Hirshfeld surface analysis

Mani Udayakumar,[a] Margarita Cerón,[b] Paulina Ceballos,[b] Judith Percino[b] and Subbiah Thamotharan[a]*

[a]Biomolecular Crystallography Laboratory, Department of Bioinformatics, School of Chemical and Biotechnology, SASTRA Deemed University, Thanjavur 613 401, India, and [b]Unidad de Polímeros y Electrónica Orgánica, Instituto de Ciencias, Benemérita Universidad Autónoma de Puebla, Val3-Ecocampus Valsequillo, Independencia O2 Sur 50, San Pedro Zacachimalpa, Puebla, CP 72960, Mexico. *Correspondence e-mail: thamu@scbt.sastra.edu

Received 21 February 2019
Accepted 16 March 2019

Edited by H. Stoeckli-Evans, University of Neuchâtel, Switzerland

Keywords: crystal structure; acrylonitrile; conjugation; hydrogen bonding; C—H···π interactions; PIXEL; Hirshfeld surface; two-dimensional fingerprint plots..

CCDC reference: 1903772

Supporting information: this article has supporting information at journals.iucr.org/e

In the solid state, the title compound, $C_{15}H_{10}ClN$, is disordered over two orientations with a refined occupancy ratio of 0.86 (2):0.14 (2). The crystal structure is mainly stabilized by intermolecular C—H···N and C—H···Cl hydrogen bonds, and C—H···π interactions. The molecules pack in columns and adjacent columns are linked by weak C—H···Cl interactions. The *PIXEL* energy analysis suggests that the intermolecular C—H···π interactions form a strong dimer in the major component. Hirshfeld analysis reveals that H···C, H···H, H···Cl and H···N contacts are the most important contributors to the crystal packing.

1. Chemical context

Acrylonitrile compounds have been used as building blocks in flavonoid pigments (Fringuelli *et al.*, 1994) and anticancer agents (Özen *et al.*, 2016). Some of these derivatives have been used to produce light-emitting diodes (LEDs) (Maruyama *et al.*, 1998; Segura *et al.*, 1999). Owing to the versatile physicochemical and biological properties of acrylonitrile derivatives, we have been investigating the optical properties of several (*Z*)-3-(substituted phenyl)-2-(pyridyl)acrylonitrile compounds with different donor and acceptor moieties (Percino *et al.*, 2010, 2011, 2014*a*,*b*, 2016*a*,*b*, 2017). Recently, we explored various (*Z*)-3-(4-halophenyl)-2-(pyridin-2/3/4-yl)acrylonitrile derivatives in order to understand the role of halogen substituents in the context of optical properties and supramolecular associations in the solid state (Venkatesan *et al.*, 2018).

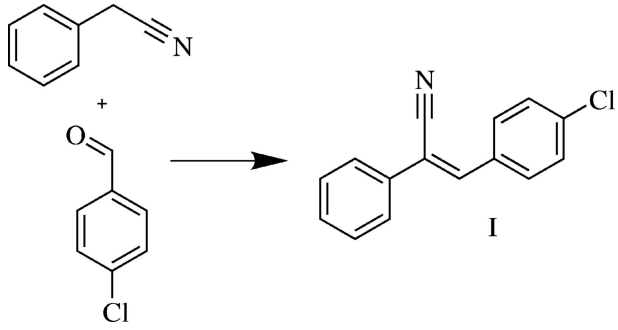

In this work, we report the synthesis and the crystal and molecular structures of an acrylonitrile derivative, namely (*Z*)-3-(4-chlorophenyl)-2-phenylacrylonitrile (**I**). We also report herein a detailed analysis of the intermolecular inter-

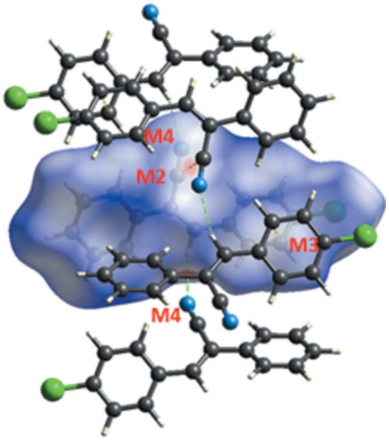

Table 1
Hydrogen-bond geometry (Å, °).

*Cg*1 and *Cg*2 are the centroids of rings C1–C6 and C9–C14 of the major disordered component. *Cg*1′ and *Cg*2′ are the centroids of rings C1′–C6′ and C9′–C14′ of the minor disordered component.

D—H···A	D—H	H···A	D···A	D—H···A
C5—H5···Cl1′^{i}	0.95	2.69	3.292 (5)	122
C8—H8···N2^{ii}	0.95	2.46	3.361 (6)	157
C8—H8···N2′^{ii}	0.95	2.53	3.44 (4)	160
C14—H14···N2′	0.95	2.54	3.22 (6)	129
C3—H3···*Cg*1^{iii}	0.95	2.99	3.860 (4)	153
C3—H3···*Cg*2′^{iii}	0.95	2.95	3.784 (9)	148
C11—H11···*Cg*2^{iv}	0.95	2.96	3.418 (7)	111
C11—H11···*Cg*1′^{iv}	0.95	2.97	3.486 (15)	115
C14—H14···*Cg*1^{v}	0.95	2.81	3.503 (3)	130
C14—H14···*Cg*2′^{v}	0.95	2.84	3.585 (8)	136
C3′—H3′···*Cg*2^{iv}	0.95	2.59	3.32 (6)	134
C3′—H3′···*Cg*1′^{iv}	0.95	2.62	3.39 (6)	139
C6′—H6′···*Cg*1^{v}	0.95	2.85	3.52 (2)	129
C6′—H6′···*Cg*2′^{v}	0.95	2.93	3.64 (2)	132

Symmetry codes: (i) $-x+1, y, -z+\frac{1}{2}$; (ii) $x-\frac{1}{2}, -y+\frac{1}{2}, -z+1$; (iii) $-x+\frac{1}{2}, y-\frac{1}{2}, z$; (iv) $-x+\frac{1}{2}, y+\frac{1}{2}, z$; (v) $-x+1, -y, -z+1$.

actions for different molecular pairs observed in **I** using the *PIXEL* method (Gavezzotti, 2002, 2011). Hirshfeld surface analysis (Spackman & Jayatilaka, 2009) was also performed to visualize the short contacts in the crystal of **I** and to determine the relative contributions of the various non-covalent interactions present in the crystal structure using two-dimensional (2D) fingerprint plots (Spackman & McKinnon, 2002; McKinnon *et al.*, 2007). We also highlight the importance of the weak halogen bonds observed in the crystal structure.

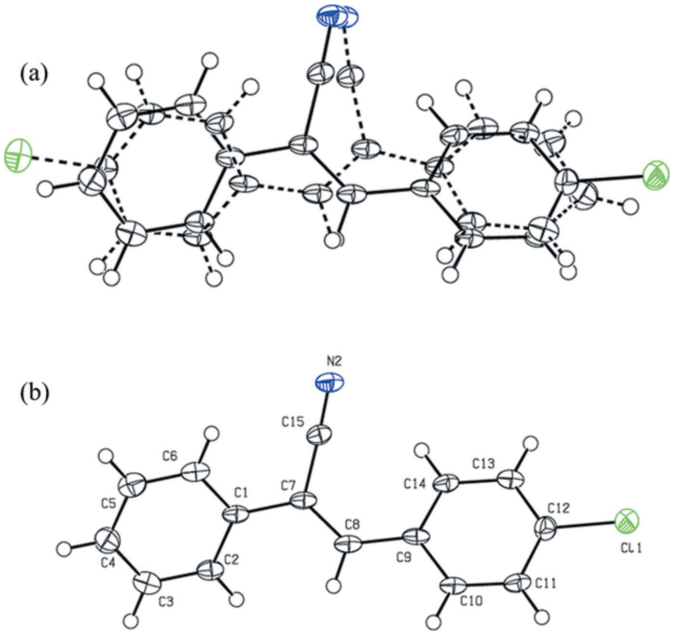

Figure 1
(*a*) The disordered components of compound **I** (major shown with solid lines and minor with broken lines) and (*b*) displacement ellipsoids of the major disordered component of **I** at the 50% pobability level, with the atom-labelling scheme.

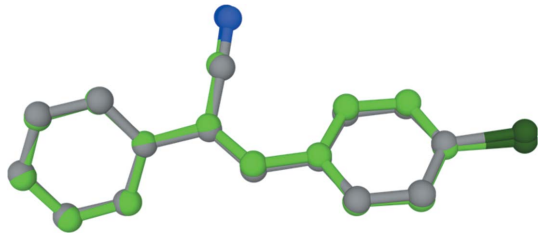

Figure 2
Structural overlay of the X-ray (grey) and optimized (green) structures.

2. Computational details

Structural optimization was carried out using *GAUSSIAN09* (Frisch *et al.*, 2013) with the M06-2X/cc-pVTZ level of theory followed by vibrational frequency calculations. The lattice and intermolecular interaction energies were calculated using the *CLP-PIXEL* program (Version 3.0; Gavezzotti, 2002, 2011). For the intermolecular interaction energy calculations, the crystal structure geometry along with normalized C—H bond lengths to their respective neutron values (Allen, 1986) was used and the electron density has been obtained at the MP2/6-31G(d,p) level of theory using *GAUSSIAN09*.

3. Structural commentary

The molecular structure of compound **I** is shown in Fig. 1. The whole molecule is disordered over two orientations with a refined occupancy ratio of 0.86 (2):0.14 (2). Only the major component is considered for further analysis and discussion. The bond lengths in **I** clearly indicate the presence of electron delocalization throughout the molecule. The geometrical features of the molecule were further analyzed using the *MOGUL* geometry check utility available in *Mercury* (Macrae *et al.*, 2008). The result suggests that the torsion angles C8—C7—C15—N2 [−166.6 (2)°] and C1—C7—C15—N2 [10.5 (2)°] are unusual. The molecule adopts a twisted conformation and the dihedral angle between the planes of the phenyl (C1–C6) and 4-chlorophenyl (C9–C14) rings is 51.91 (8)°. When the unsubstituted phenyl ring in **I** was

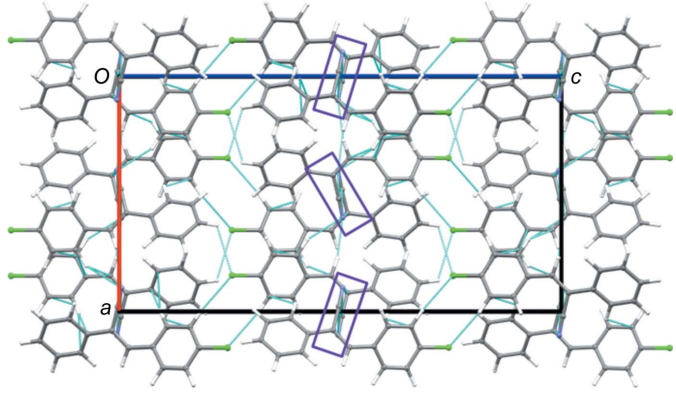

Figure 3
A view along the *b* axis of the crystal packing of compound **I**, showing the nitrile stacking in the purple rectangles.

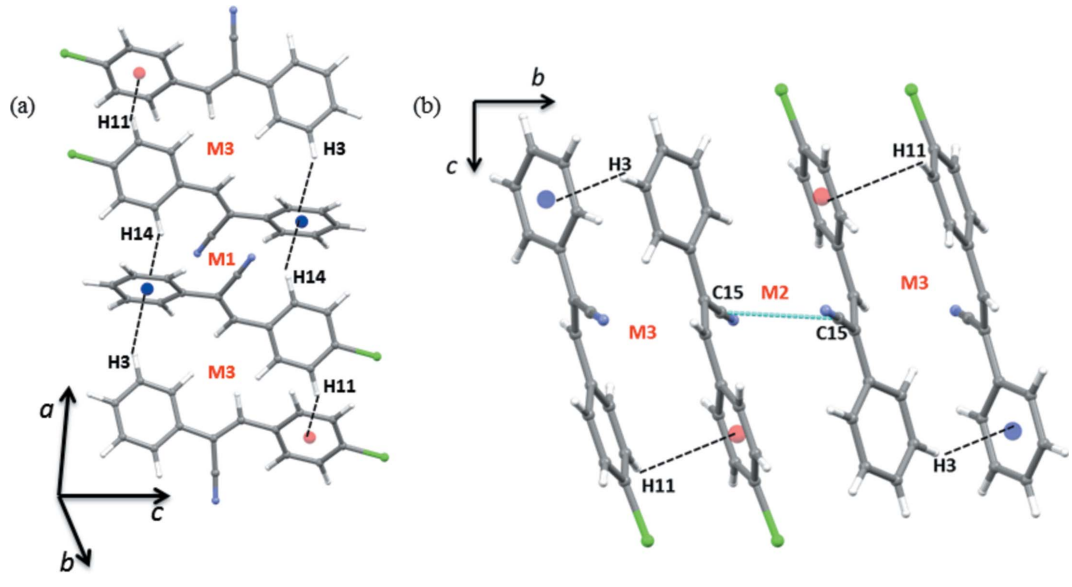

Figure 4
(*a*) The molecular chain generated by intermolecular C—H···π interactions (motif sequence M3···M1···M3) and (*b*) adjacent M3 motifs interlinked by nitrile–nitrile stacking (motif M2). The centroids are shown as small spheres (*Cg*1 blue and *Cg*2 red).

replaced by a pyridine ring (Venkatesan *et al.*, 2018), the molecular twist was reduced by at least 50%, and in pyridine containing compounds, the dihedral angles between the two rings are in a range of *ca* 1–27° (Cambridge Structural Database; Groom *et al.*, 2016).

To understand the conformational flexibility of **I**, we performed a structural optimization using the *GAUSSIAN09* program (Frisch *et al.*, 2013), without any constraints. The vibrational frequency calculation confirmed that the optimized structure is found to be the true energy minima on the potential energy surface, since there were no negative frequencies observed for the optimized geometries. The X-ray and optimized structures superimpose well, with an r.m.s. deviation of 0.13 Å (Fig. 2).

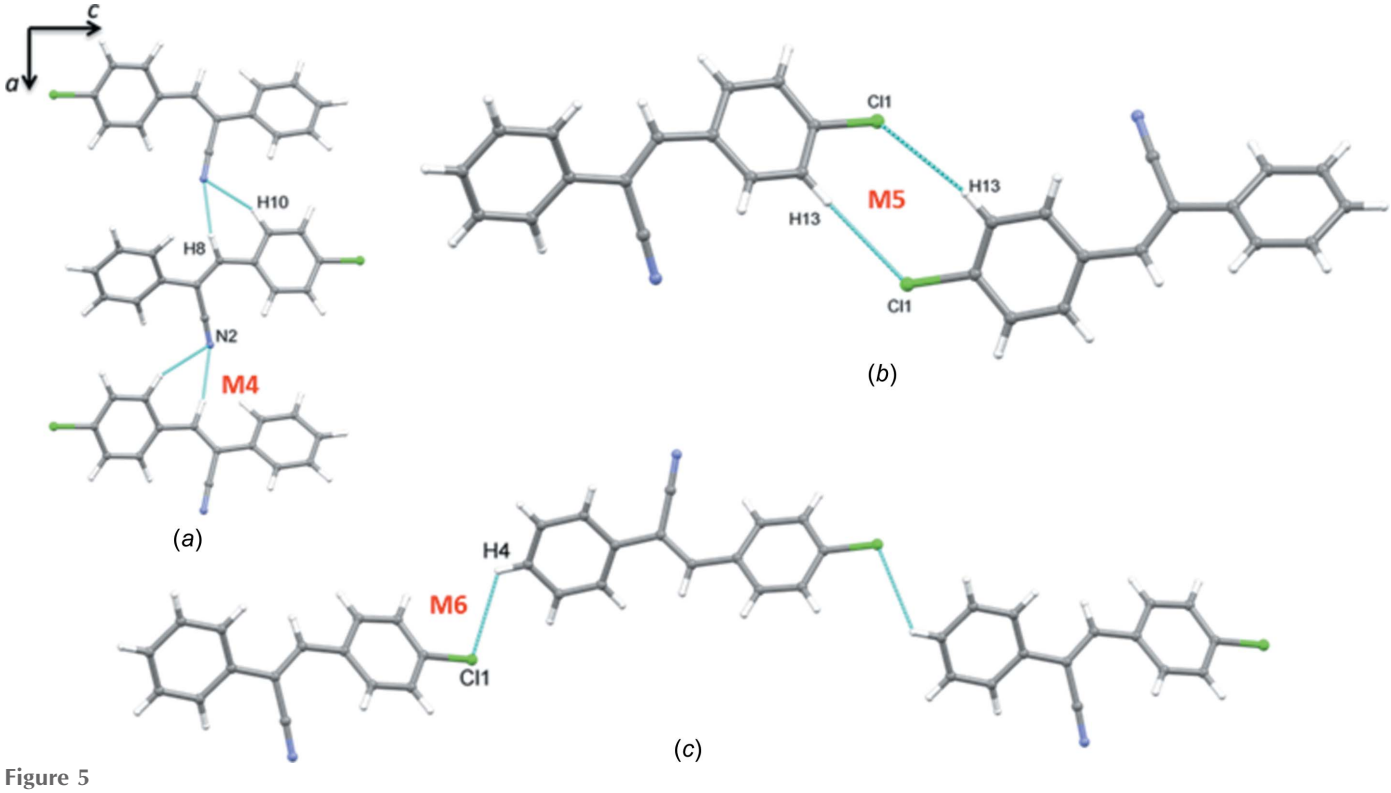

Figure 5
(*a*) The molecular chain formed by three-centred C—H···N interactions, (*b*) a closed molecular dimer generated by intermolecular C—H···Cl interactions and (*c*) a *C*(12) chain formed by intermolecular C—H···Cl interactions.

Table 2
Intermolecular interaction energies (in kcal mol^{-1}) for different molecular pairs observed in the major component of the title compound; CD is the centroid-to-centroid distance.

Motif	CD (Å)	Symmetry	E_{Coul}	E_{pol}	$E_{energy\text{-}dispersive}$	E_{rep}	E_{tot}	Possible interactions	Geometry (Å, °)[a]
M1	5.163	$-x+1, -y, -z+1$	−4.0	−1.4	−12.5	8.3	−9.5	C14—H14···*Cg*1	2.81, 130
M2	4.820	$-x+1, -y+1, -z+1$	−3.1	−1.5	−11.5	7.4	−8.7	C15···C15(π–π)	3.274 (4)
M3	5.122	$-x+\frac{1}{2}, y-\frac{1}{2}, z$	−1.9	−1.0	−10.0	5.6	−7.3	C3—H3···*Cg*1	2.99, 153
		$-x+\frac{1}{2}, y+\frac{1}{2}, z$						C11—H11···*Cg*2	2.96, 111
M4	6.925	$x-\frac{1}{2}, -y+\frac{1}{2}, -z+1$	−4.3	−1.6	−5.2	5.3	−5.9	C8—H8···N2	2.34, 156
								C10—H10···N2	2.66, 143
M5	11.134	$-x+1, y, -z+\frac{3}{2}$	−1.1	−0.5	−3.2	1.8	−2.8	C13—H13···Cl1	2.95, 152
M6	13.104	$-x+\frac{1}{2}, -y+\frac{1}{2}, z-\frac{1}{2}$	−0.6	−0.4	−2.8	2.1	−1.6	C4—H4···Cl1	2.98, 114

Note: (*a*) neutron values are given for all *D*—H···*A* interactions.

4. Supramolecular features

In the crystal, molecules are arranged in a columnar packing mode *via* intermolecular C—H···π, C—H···N and C—H···Cl interactions (Table 1 and Fig. 3). Adjacent columns are interconnected by halogen bonds (C—H···Cl). Within the column, there is nitrile–nitrile stacking and molecules are interlinked by C—H···π and C—H···N interactions (Table 1).

5. Lattice and intermolecular interaction energies

The lattice energy calculations reveal that the crystal packing is predominantly stabilized through dispersion energy (71%) and the electrostatic (Coulombic + polarization) energy contributes 29% towards the stabilization of the crystal structure. The total lattice energy (−28.9 kcal mol^{-1}) is the sum of the Coulombic (−10.5 kcal mol^{-1}), polarization (−4.7 kcal mol^{-1}), dispersion (−36.6 kcal mol^{-1}) and repulsion (22.9 kcal mol^{-1}) terms. Furthermore, different motifs formed in the major component of **I** and their energetics are discussed below (Table 2).

Inversion-related molecules form the strongest dimer (motif M1) which is held by intermolecular C—H···π interactions with an interaction energy of −9.5 kcal mol^{-1}. As expected, the dispersion contribution (70%) is more significant towards the stabilization of this dimer. Further, this dimer is flanked on both sides by other molecules. As shown in Fig. 4(*a*), these molecules interact with the central dimer (motif M1) through two C—H···π interactions (motif M3; interaction energy = −7.3 kcal mol^{-1}). It is to be noted that the motif M3 is more dispersive in nature (78%) than motif M1. The nitrile group of one molecule stacks with the nitrile group of an inversion-related molecule (motif M2; interaction energy = −8.7 kcal mol^{-1} and 71% dispersion contribution). The shortest distance observed between two C15 atoms is 3.274 (4) Å and the motif M2 is also flanked on both sides by motif M3. These motifs act together to link the molecules into a chain which runs parallel to the *b* axis (Fig. 4*b*).

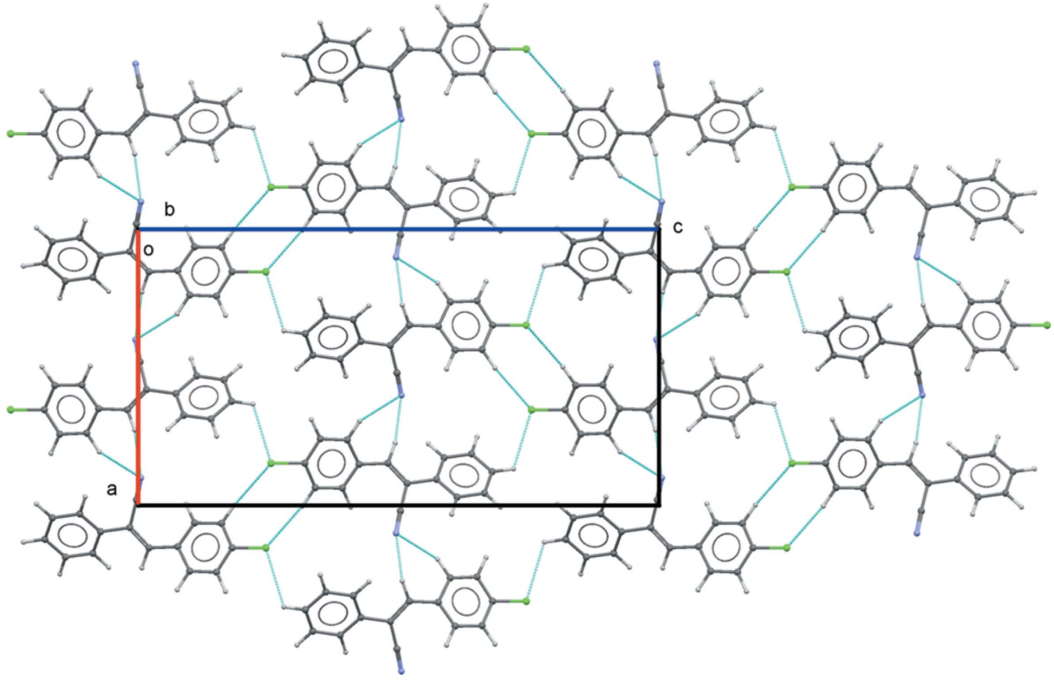

Figure 6
The molecular sheet assembled by intermolecular C—H···N and C—H···Cl interactions.

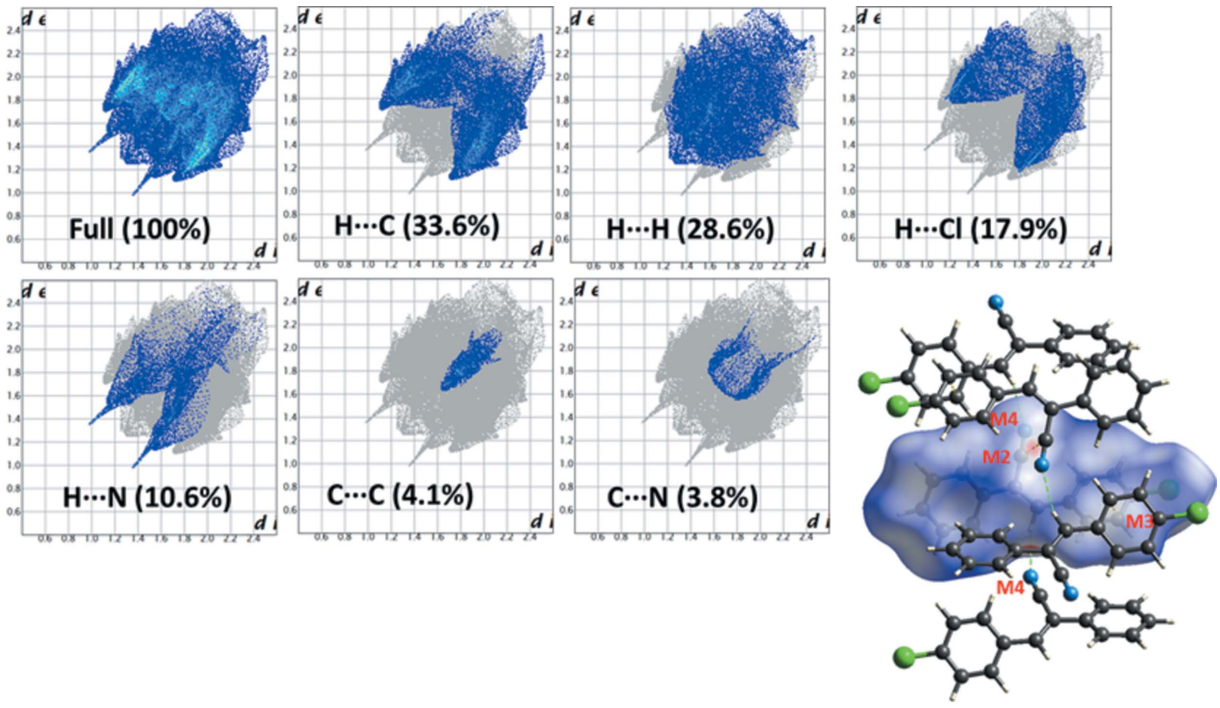

Figure 7
2D fingerprint plots for different intermolecular contacts and the Hirshfeld surface mapped over d_{norm} to hightlight the short intermolecular contacts for the major disordered component of **I**.

Motif M4 (interaction energy = −5.9 kcal mol^{-1}) is stabilized by three-centred intermolecular C—H···N interactions in which the nitrile N atom acts as an acceptor and the vinylic proton (H9) and one of the protons (H10) of chlorophenyl ring are involved as donors (Fig. 5). These three-centred interactions link the molecules into a chain which runs parallel to the *a* axis. 53% of the electrostatic and 47% of the dispersion energy contribute towards stabilization of motif M4.

The energetically least-stable dimers (motifs M5 and M6) are formed by intermolecular C—H···Cl interactions (Fig. 5). These two interactions help to link adjacent columns in the crystal, as mentioned above. The molecules form an $R_2^2(8)$ loop in the case of motif M5, with an interaction energy of −2.8 kcal mol^{-1}. We note that the dispersion energy (67%) contributes nearly double that of the electrostatic energy (33%) for the stabilization of this motif. Further, a molecular chain is related to motif M6 (interaction energy = −1.6 kcal mol^{-1}) propagating along the *c* axis direction. This dimer is more dispersive in nature and 75% of the dispersion energy contributes towards the stabilization. Motifs M4–M6 combine to form sheets parallel to the *ac* plane (Fig. 6).

6. Hirshfeld surface analysis and 2D fingerprint plots

The Hirshfeld surface analysis (Spackman & Jayatilaka, 2009) and the associated 2D fingerprint plots (McKinnon *et al.*, 2007) were performed with *CrystalExplorer17* (Turner *et al.*, 2017) for both the major and the minor disordered components. For each component, the occupancies of all atoms were made equal to 1. Hirshfeld surface (HS) analysis was carried out in order to gain more insight into the nature and extent of the intermolecular interactions and to quantify the relative contributions of the different non-covalent interactions that exist in the crystal. The HS surface was mapped over d_{norm} and the diagram reveals that motifs M2 and M4 are visible as red spots on the HS (Fig. 7) in the major disordered component. It is to be noted that a pale-red spot is noticed for motif M3 when compared to the other two motifs. As mentioned above, motif M4 has two intermolecular C—H···N interactions and one of them is found to be a close contact (C8—H8···N2).

2D fingerprint plots for the major and the minor components are illustrated in Figs. 7 and 8. For the major component of **I**, it is found that the contributions for the H···C (33.6%) and H···H (28.6%) contacts are relatively high in comparison to other non-covalent interactions (Fig. 7). It is of interest to note that the H···Cl contacts also contribute substantially (17.9%) to the crystal packing. As noted above, neighbouring columns are interlinked in the crystal *via* intermolecular H···Cl contacts. The intermolecular H···N contacts contribute 10.6% towards the crystal packing. The other contacts, such as C···C (4.1%) and C···N (3.8%), also supplement the overall crystal packing. The former contact represents the motifs M2 and M3, while the latter contact is mainly due to the stacking of the nitrile groups.

In the case of the minor component, the relative contributions of some of the intermolecular contacts are very similar to those for the major component, as shown in Fig. 8. However, the H···Cl contacts are reduced by 4.9%. This difference clearly indicates the importance of halogen interactions in the major component of the title compound.

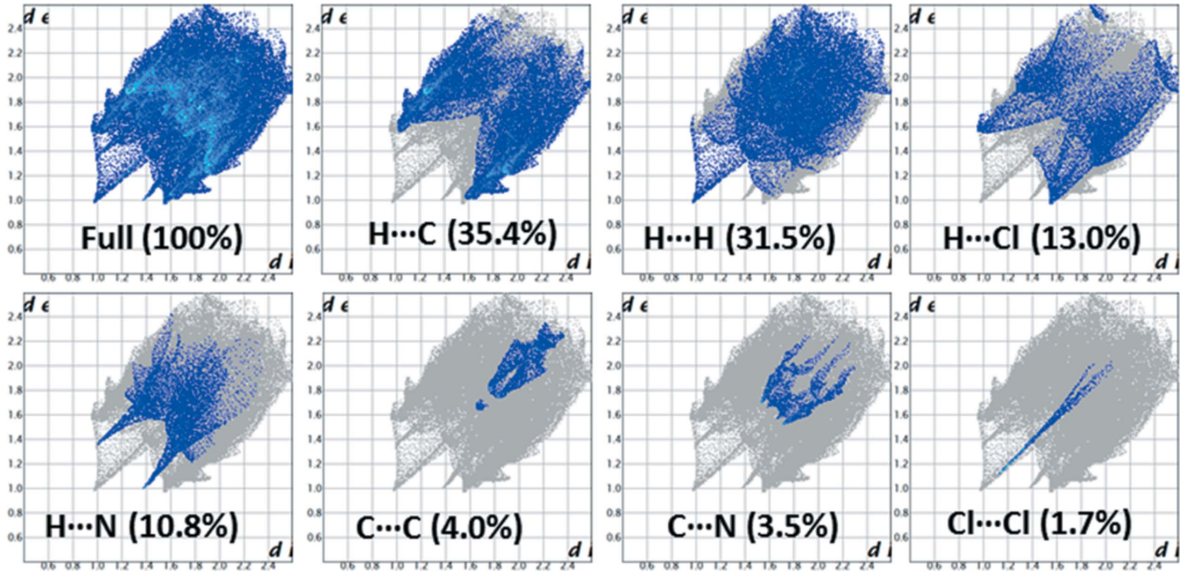

Figure 8
2D fingerprint plots for the different intermolecular contacts and their relative contributions for the minor disordered component of **I**.

7. Database survey

A search of the Cambridge Structural Database (CSD, Version 5.40, update of February 2019; Groom *et al.*, 2016) using the (*Z*)-2,3-diphenylacrylonitrile skeleton yielded 306 hits, which include multiple reports of a number of structures. Limiting the search to structures with a halogen atom attached to the phenyl ring, as in the title compound, yielded 13 hits. Two structures are similar to the title compound, namely 2-(4-aminophenyl)-3-(4-bromophenyl)acrylonitrile (CSD refcode IYIBOJ; Bai *et al.*, 2016) and (*Z*)-3-(2-chloro-6-fluorophenyl)-2-(4-methoxyphenyl)acrylonitrile (KEVQOS; Naveen *et al.*, 2006). Here the planes of the aryl rings are inclined to each other by 66.16 (13)° in IYIBOJ and 57.43 (19)° in KEVQOS. In **I**, this dihedral angle is 51.91 (8)° in the major disordered component and 61.8 (13)° in the minor disordered component.

Table 3
Experimental details.

Crystal data	
Chemical formula	$C_{15}H_{10}ClN$
M_r	239.69
Crystal system, space group	Orthorhombic, *Pbcn*
Temperature (K)	100
a, *b*, *c* (Å)	13.3417 (8), 7.1030 (5), 25.1418 (18)
V (Å^3)	2382.6 (3)
Z	8
Radiation type	Cu *Kα*
μ (mm^{-1})	2.61
Crystal size (mm)	0.31 × 0.29 × 0.05
Data collection	
Diffractometer	SuperNova, Dual, Cu at zero, Atlas
Absorption correction	Analytical (*CrysAlis PRO*; Agilent, 2012)
T_{min}, T_{max}	0.560, 0.889
No. of measured, independent and observed [$I > 2\sigma(I)$] reflections	6681, 2132, 1930
R_{int}	0.031
$(\sin \theta/\lambda)_{max}$ (Å^{-1})	0.598
Refinement	
$R[F^2 > 2\sigma(F^2)]$, $wR(F^2)$, *S*	0.050, 0.122, 1.10
No. of reflections	2132
No. of parameters	212
No. of restraints	44
H-atom treatment	H-atom parameters constrained
$\Delta\rho_{max}$, $\Delta\rho_{min}$ (e Å^{-3})	0.28, −0.20

Computer programs: *CrysAlis PRO* (Agilent, 2012), *SHELXS2013* (Sheldrick, 2008), *SHELXL2014* (Sheldrick, 2015), *PLATON* (Spek, 2009), *Mercury* (Macrae *et al.*, 2008) and *publCIF* (Westrip, 2010).

8. Synthesis and crystallization

A mixture of phenylacetonitrile (0.53 ml, 4.6 mmol) and 4-chlorobenzaldehyde (4.6 mmol, 0.65 g) was stirred at room temperature for 10 min. Subsequently, the temperature was increased gradually to 403 K and maintained at that temperature for 39 h. Initially, the mixture was colourless and then became viscous and dark. This viscous solution was cooled, treated with hexane and finally filtered. The filtrate contained small colourless crystals. Further purification of the title compound (yield 83%, m.p. 368–370 K) was carried out by recrystallization from hexane. Colourless plate-like crystals, suitable for X-ray diffraction analysis, were obtained by slow evaporation of a solution of **I** in ethanol at 277 K after a period of 7 d.

9. Refinement

Crystal data, data collection and structure refinement details are summarized in Table 3. The whole molecule was disordered and the major and minor components of the disorder refined to 0.86 (2) and 0.14 (2), respectively. All H atoms were placed in calculated positions and treated as riding, with C—H = 0.95 Å and $U_{iso}(H) = 1.2U_{eq}(C)$.

Acknowledgements

The authors would like to thank Laboratorio Nacional de Supercoìmputo del Sureste (LNS–BUAP) for the calculus service and the PEZM NAT17-G (VIEP–BUAP) and SA/103.5/15/12684 (PRODEP–SEP) projects, as well as Dr Maxime A. Siegler (Johns Hopkins University) for assistance with the data collection. ST thanks the DST–SERB for financial support.

References

Agilent (2012). *CrysAlis PRO*. Agilent Technologies, Yarnton, Oxfordshire, England.

Allen, F. H. (1986). *Acta Cryst.* B**42**, 515–522.

Bai, X.-Y., Shi, C.-C., Sun, Y., Ding, R., Huang, J.-Y. & Yang, J.-X. (2016). *Jiegou Huaxue (Chin.) (Chin. J. Struct. Chem.)*, **35**, 1362–1368.

Fringuelli, F., Pani, G., Piermatti, O. & Pizzo, F. (1994). *Tetrahedron*, **50**, 11499–11508.

Frisch, M. J., *et al.* (2013). *GAUSSIAN09*. Revision D.01. Gaussian Inc., Wallingford, CT, USA.

Gavezzotti, A. (2002). *J. Phys. Chem. B*, **106**, 4145–4154.

Gavezzotti, A. (2011). *New J. Chem.* **35**, 1360–1368.

Groom, C. R., Bruno, I. J., Lightfoot, M. P. & Ward, S. C. (2016). *Acta Cryst.* B**72**, 171–179.

Macrae, C. F., Bruno, I. J., Chisholm, J. A., Edgington, P. R., McCabe, P., Pidcock, E., Rodriguez-Monge, L., Taylor, R., van de Streek, J. & Wood, P. A. (2008). *J. Appl. Cryst.* **41**, 466–470.

Maruyama, S., Tao, X. T., Hokari, H., Noh, T., Zhang, Y., Wada, T. & Miyata, S. (1998). *Chem. Lett.* **27**, 749–750.

McKinnon, J. J., Jayatilaka, D. & Spackman, M. A. (2007). *Chem. Commun.* pp. 3814–3816.

Naveen, S., Kavitha, C. V., Sarala, G., Anandalwar, S. M., Prasad, J. S. & Rangappa, K. S. (2006). *Anal. Sci. X-ray Struct. Anal. Online*, **22**, x291.

Özen, F., Tekin, S., Koran, K., Sandal, S. & Görgülü, A. O. (2016). *Appl. Biol. Chem.* **59**, 239–248.

Percino, J., Ceroń, M., Venkatesan, P., Ceballos, P., Bañuelos, A., Rodríguez, O., Siegler, M. A., Robles, F., Chapela, V. M., Soriano-Moro, G., Peŕez-Gutieŕrez, E., Bonilla-Cruz, J. & Thamotharan, S. (2017). *Cryst. Growth Des.* **17**, 1679–1694.

Percino, M. J., Cerón, M., Castro, M. E., Soriano-Moro, G., Chapela, V. M. & Meléndez, F. J. (2014*a*). *Chem. Pap.* **68**, 668–680.

Percino, M. J., Cerón, M., Ceballos, P., Soriano-Moro, G., Castro, M. E., Chapela, V. M., Bonilla-Cruz, J., Reyes-Reyes, M., López-Sandoval, R. & Siegler, M. A. (2014*b*). *J. Mol. Struct.* **1078**, 74–82.

Percino, M. J., Cerón, M., Ceballos, P., Soriano-Moro, G., Rodriguez, O., Chapela, V. M., Castro, M. E., Bonilla-Cruz, J. & Siegler, M. A. (2016*b*). *CrystEngComm*, **18**, 7554–7572.

Percino, M. J., Cerón, M., Rodríguez, O., Soriano-Moro, G., Castro, M. E., Chapela, V. M., Siegler, M. A. & Pérez-Gutiérrez, E. (2016*a*). *Molecules*, **21**, 389.

Percino, M. J., Chapela, V. M., Montiel, L.-F., Pérez-Gutiérrez, E. & Maldonado, J. L. (2010). *Chem. Pap.* **64**, 360–367.

Percino, M. J., Chapela, V. M., Pérez-Gutiérrez, E., Cerón, M. & Soriano, G. (2011). *Chem. Pap.* **65**, 42–51.

Segura, J. L., Martín, N. & Hanack, M. (1999). *Eur. J. Org. Chem.* **3**, 643–651.

Sheldrick, G. M. (2008). *Acta Cryst.* A**64**, 112–122.

Sheldrick, G. M. (2015). *Acta Cryst.* C**71**, 3–8.

Spackman, M. A. & Jayatilaka, D. (2009). *CrystEngComm*, **11**, 19–32.

Spackman, M. A. & McKinnon, J. J. (2002). *CrystEngComm*, **4**, 378–392.

Spek, A. L. (2009). *Acta Cryst.* D**65**, 148–155.

Turner, M. J., McKinnon, J. J., Wolff, S. K., Grimwood, D. J., Spackman, P. R., Jayatilaka, D. & Spackman, M. A. (2017). *CrystalExplorer17*. University of Western Australia.

Venkatesan, P., Cerón, M., Thamotharan, S., Robles, F. & Percino, M. J. (2018). *CrystEngComm*, **20**, 7554–7572.

Westrip, S. P. (2010). *J. Appl. Cryst.* **43**, 920–925.

supporting information

Acta Cryst. (2019). E**75**, 499-505 [https://doi.org/10.1107/S2056989019003694]

Quantitative analysis of weak non-covalent interactions in (*Z*)-3-(4-chlorophenyl)-2-phenylacrylonitrile: insights from *PIXEL* and Hirshfeld surface analysis

Mani Udayakumar, Margarita Cerón, Paulina Ceballos, Judith Percino and Subbiah Thamotharan

Computing details

Data collection: (*CrysAlis PRO*; Agilent, 2012); cell refinement: (*CrysAlis PRO*; Agilent, 2012); data reduction: (*CrysAlis PRO*; Agilent, 2012); program(s) used to solve structure: *SHELXS2013* (Sheldrick, 2008); program(s) used to refine structure: *SHELXL2014*/7 (Sheldrick, 2015); molecular graphics: *PLATON* (Spek, 2009) and *Mercury* (Macrae *et al.*, 2008); software used to prepare material for publication: *publCIF* (Westrip, 2010).

(*Z*)-3-(4-Chlorophenyl)-2-phenylacrylonitrile

Crystal data

$C_{15}H_{10}ClN$
M_r = 239.69
Orthorhombic, *Pbcn*
a = 13.3417 (8) Å
b = 7.1030 (5) Å
c = 25.1418 (18) Å
V = 2382.6 (3) Å^3
Z = 8
F(000) = 992
D_x = 1.336 Mg m^{-3}
Cu $K\alpha$ radiation, λ = 1.54178 Å
Cell parameters from 3085 reflections
θ = 4.8–67.4°
μ = 2.61 mm^{-1}
T = 100 K
Plate, colourless
0.31 × 0.29 × 0.05 mm

Data collection

SuperNova, Dual, Cu at zero, Atlas diffractometer
Radiation source: SuperNova (Cu) X-ray Source
ω scans
Absorption correction: analytical (CrysAlisPro; Agilent, 2012)
T_{min} = 0.560, T_{max} = 0.889
6681 measured reflections
2132 independent reflections
1930 reflections with $I > 2\sigma(I)$
R_{int} = 0.031
θ_{max} = 67.3°, θ_{min} = 3.5°
h = −15→11
k = −6→8
l = −23→30

Refinement

Refinement on F^2
Least-squares matrix: full
$R[F^2 > 2\sigma(F^2)]$ = 0.050
$wR(F^2)$ = 0.122
S = 1.10
2132 reflections
212 parameters
44 restraints
Primary atom site location: structure-invariant direct methods
Secondary atom site location: difference Fourier map
Hydrogen site location: inferred from neighbouring sites

H-atom parameters constrained
$w = 1/[\sigma^2(F_o^2) + (0.0441P)^2 + 2.5669P]$
where $P = (F_o^2 + 2F_c^2)/3$

$(\Delta/\sigma)_{max} = 0.001$
$\Delta\rho_{max} = 0.28$ e Å^{-3}
$\Delta\rho_{min} = -0.20$ e Å^{-3}

Special details

Geometry. All esds (except the esd in the dihedral angle between two l.s. planes) are estimated using the full covariance matrix. The cell esds are taken into account individually in the estimation of esds in distances, angles and torsion angles; correlations between esds in cell parameters are only used when they are defined by crystal symmetry. An approximate (isotropic) treatment of cell esds is used for estimating esds involving l.s. planes.

Fractional atomic coordinates and isotropic or equivalent isotropic displacement parameters (Å²)

	x	*y*	*z*	U_{iso}*/U_{eq}	Occ. (<1)
Cl1	0.34667 (5)	0.49268 (11)	0.74493 (3)	0.0369 (2)	0.8598 (17)
C12	0.3468 (2)	0.4040 (5)	0.68021 (11)	0.0258 (7)	0.8598 (17)
C11	0.2585 (4)	0.4067 (10)	0.65042 (19)	0.0251 (12)	0.8598 (17)
H11	0.1975	0.4506	0.6654	0.030*	0.8598 (17)
C10	0.26234 (19)	0.3441 (7)	0.59886 (15)	0.0230 (8)	0.8598 (17)
H10	0.2031	0.3475	0.5779	0.028*	0.8598 (17)
C9	0.35071 (18)	0.2756 (4)	0.57609 (11)	0.0211 (6)	0.8598 (17)
C14	0.43690 (19)	0.2651 (4)	0.60818 (12)	0.0238 (6)	0.8598 (17)
H14	0.4969	0.2135	0.5940	0.029*	0.8598 (17)
C13	0.4351 (2)	0.3289 (4)	0.66008 (13)	0.0251 (6)	0.8598 (17)
H13	0.4935	0.3215	0.6817	0.030*	0.8598 (17)
C8	0.34672 (17)	0.2150 (4)	0.52053 (11)	0.0221 (6)	0.8598 (17)
H8	0.2831	0.1722	0.5086	0.026*	0.8598 (17)
C7	0.41994 (17)	0.2112 (3)	0.48387 (10)	0.0209 (5)	0.8598 (17)
C15	0.52002 (18)	0.2729 (4)	0.49672 (11)	0.0223 (6)	0.8598 (17)
C1	0.4052 (2)	0.1547 (4)	0.42761 (11)	0.0221 (6)	0.8598 (17)
C2	0.3269 (2)	0.0340 (5)	0.41280 (15)	0.0243 (7)	0.8598 (17)
H2	0.2827	−0.0136	0.4392	0.029*	0.8598 (17)
C3	0.3133 (3)	−0.0165 (6)	0.36020 (18)	0.0295 (7)	0.8598 (17)
H3	0.2595	−0.0976	0.3508	0.035*	0.8598 (17)
C4	0.3776 (2)	0.0501 (5)	0.32082 (12)	0.0316 (8)	0.8598 (17)
H4	0.3685	0.0140	0.2848	0.038*	0.8598 (17)
C5	0.4552 (2)	0.1704 (5)	0.33516 (12)	0.0319 (7)	0.8598 (17)
H5	0.4989	0.2181	0.3086	0.038*	0.8598 (17)
C6	0.46955 (19)	0.2214 (4)	0.38776 (13)	0.0258 (6)	0.8598 (17)
H6	0.5235	0.3024	0.3969	0.031*	0.8598 (17)
N2	0.6003 (4)	0.322 (2)	0.5051 (3)	0.0275 (13)	0.8598 (17)
Cl1′	0.4211 (3)	−0.0021 (6)	0.26712 (16)	0.0355 (12)	0.1402 (17)
C12′	0.3955 (15)	0.065 (3)	0.3320 (6)	0.0258 (7)	0.1402 (17)
C11′	0.3213 (17)	−0.031 (3)	0.3605 (10)	0.0251 (12)	0.1402 (17)
H11′	0.2808	−0.1233	0.3438	0.030*	0.1402 (17)
C10′	0.3084 (15)	0.012 (3)	0.4131 (9)	0.0230 (8)	0.1402 (17)
H10′	0.2584	−0.0516	0.4330	0.028*	0.1402 (17)
C9′	0.3673 (11)	0.148 (2)	0.4380 (6)	0.0211 (6)	0.1402 (17)
C14′	0.4402 (11)	0.240 (2)	0.4083 (7)	0.0238 (6)	0.1402 (17)
H14′	0.4806	0.3321	0.4253	0.029*	0.1402 (17)

C13′	0.4562 (13)	0.202 (2)	0.3551 (8)	0.0251 (6)	0.1402 (17)
H13′	0.5062	0.2656	0.3352	0.030*	0.1402 (17)
C8′	0.3491 (12)	0.192 (2)	0.4942 (5)	0.0221 (6)	0.1402 (17)
H8′	0.2817	0.1744	0.5054	0.026*	0.1402 (17)
C7′	0.4111 (9)	0.251 (2)	0.5321 (5)	0.0209 (5)	0.1402 (17)
C15′	0.5165 (10)	0.281 (3)	0.5210 (7)	0.0223 (6)	0.1402 (17)
C1′	0.3810 (13)	0.294 (3)	0.5875 (6)	0.0221 (6)	0.1402 (17)
C2′	0.2837 (15)	0.357 (5)	0.6003 (10)	0.0243 (7)	0.1402 (17)
H2′	0.2315	0.3515	0.5746	0.029*	0.1402 (17)
C3′	0.265 (3)	0.429 (9)	0.6513 (12)	0.0295 (7)	0.1402 (17)
H3′	0.2066	0.5025	0.6568	0.035*	0.1402 (17)
C4′	0.3293 (16)	0.396 (4)	0.6948 (8)	0.0316 (8)	0.1402 (17)
H4′	0.3103	0.4223	0.7305	0.038*	0.1402 (17)
C5′	0.4215 (14)	0.322 (3)	0.6819 (7)	0.0319 (7)	0.1402 (17)
H5′	0.4684	0.2946	0.7093	0.038*	0.1402 (17)
C6′	0.4461 (14)	0.288 (3)	0.6300 (8)	0.0258 (6)	0.1402 (17)
H6′	0.5140	0.2566	0.6225	0.031*	0.1402 (17)
N2′	0.598 (3)	0.323 (14)	0.514 (3)	0.0275 (13)	0.1402 (17)

Atomic displacement parameters (Å²)

	U^{11}	U^{22}	U^{33}	U^{12}	U^{13}	U^{23}
Cl1	0.0262 (4)	0.0535 (5)	0.0309 (4)	0.0039 (3)	0.0002 (2)	−0.0111 (3)
C12	0.0270 (15)	0.0252 (14)	0.0252 (16)	0.0003 (12)	0.0022 (11)	−0.0039 (13)
C11	0.0152 (15)	0.023 (3)	0.0373 (14)	0.0016 (17)	0.0025 (11)	0.0000 (13)
C10	0.0133 (15)	0.0221 (16)	0.0336 (13)	−0.0006 (15)	−0.0016 (13)	0.0021 (11)
C9	0.0133 (13)	0.0151 (12)	0.0348 (14)	−0.0033 (11)	−0.0009 (10)	0.0039 (11)
C14	0.0145 (13)	0.0231 (14)	0.0339 (15)	0.0026 (10)	0.0024 (13)	0.0000 (13)
C13	0.0168 (12)	0.0252 (14)	0.0335 (16)	−0.0012 (10)	−0.0025 (12)	0.0013 (14)
C8	0.0137 (11)	0.0163 (12)	0.0362 (15)	0.0001 (9)	−0.0004 (12)	0.0033 (12)
C7	0.0130 (11)	0.0159 (11)	0.0336 (12)	0.0010 (9)	−0.0010 (9)	0.0034 (10)
C15	0.0178 (12)	0.0200 (12)	0.0290 (14)	0.0022 (9)	0.0022 (11)	0.0019 (13)
C1	0.0134 (12)	0.0197 (13)	0.0332 (14)	0.0021 (12)	−0.0008 (10)	0.0021 (11)
C2	0.0190 (17)	0.0195 (15)	0.0344 (14)	−0.0013 (12)	0.0006 (13)	0.0025 (11)
C3	0.0250 (16)	0.0279 (17)	0.0355 (15)	−0.0025 (13)	−0.0046 (12)	0.0017 (12)
C4	0.0303 (17)	0.0355 (17)	0.0289 (16)	0.0033 (13)	−0.0026 (12)	0.0013 (13)
C5	0.0269 (14)	0.0346 (17)	0.0343 (16)	0.0020 (13)	0.0021 (13)	0.0059 (13)
C6	0.0173 (13)	0.0228 (14)	0.0372 (17)	−0.0004 (11)	0.0009 (11)	0.0051 (12)
N2	0.0163 (10)	0.0277 (10)	0.039 (4)	0.0005 (8)	0.0000 (12)	0.000 (3)
Cl1′	0.042 (2)	0.036 (2)	0.029 (2)	0.0029 (19)	0.0032 (17)	−0.0018 (17)
C12′	0.0270 (15)	0.0252 (14)	0.0252 (16)	0.0003 (12)	0.0022 (11)	−0.0039 (13)
C11′	0.0152 (15)	0.023 (3)	0.0373 (14)	0.0016 (17)	0.0025 (11)	0.0000 (13)
C10′	0.0133 (15)	0.0221 (16)	0.0336 (13)	−0.0006 (15)	−0.0016 (13)	0.0021 (11)
C9′	0.0133 (13)	0.0151 (12)	0.0348 (14)	−0.0033 (11)	−0.0009 (10)	0.0039 (11)
C14′	0.0145 (13)	0.0231 (14)	0.0339 (15)	0.0026 (10)	0.0024 (13)	0.0000 (13)
C13′	0.0168 (12)	0.0252 (14)	0.0335 (16)	−0.0012 (10)	−0.0025 (12)	0.0013 (14)
C8′	0.0137 (11)	0.0163 (12)	0.0362 (15)	0.0001 (9)	−0.0004 (12)	0.0033 (12)
C7′	0.0130 (11)	0.0159 (11)	0.0336 (12)	0.0010 (9)	−0.0010 (9)	0.0034 (10)

C15′	0.0178 (12)	0.0200 (12)	0.0290 (14)	0.0022 (9)	0.0022 (11)	0.0019 (13)
C1′	0.0134 (12)	0.0197 (13)	0.0332 (14)	0.0021 (12)	−0.0008 (10)	0.0021 (11)
C2′	0.0190 (17)	0.0195 (15)	0.0344 (14)	−0.0013 (12)	0.0006 (13)	0.0025 (11)
C3′	0.0250 (16)	0.0279 (17)	0.0355 (15)	−0.0025 (13)	−0.0046 (12)	0.0017 (12)
C4′	0.0303 (17)	0.0355 (17)	0.0289 (16)	0.0033 (13)	−0.0026 (12)	0.0013 (13)
C5′	0.0269 (14)	0.0346 (17)	0.0343 (16)	0.0020 (13)	0.0021 (13)	0.0059 (13)
C6′	0.0173 (13)	0.0228 (14)	0.0372 (17)	−0.0004 (11)	0.0009 (11)	0.0051 (12)
N2′	0.0163 (10)	0.0277 (10)	0.039 (4)	0.0005 (8)	0.0000 (12)	0.000 (3)

Geometric parameters (Å, º)

Cl1—C12	1.745 (3)	Cl1′—Cl1′^{i}	2.275 (9)
C12—C13	1.389 (4)	C12′—C13′	1.389 (17)
C12—C11	1.397 (5)	C12′—C11′	1.399 (18)
C11—C10	1.371 (4)	C11′—C10′	1.368 (19)
C11—H11	0.9500	C11′—H11′	0.9500
C10—C9	1.398 (4)	C10′—C9′	1.391 (17)
C10—H10	0.9500	C10′—H10′	0.9500
C9—C14	1.407 (4)	C9′—C14′	1.388 (15)
C9—C8	1.462 (4)	C9′—C8′	1.467 (15)
C14—C13	1.382 (4)	C14′—C13′	1.383 (16)
C14—H14	0.9500	C14′—H14′	0.9500
C13—H13	0.9500	C13′—H13′	0.9500
C8—C7	1.344 (3)	C8′—C7′	1.331 (14)
C8—H8	0.9500	C8′—H8′	0.9500
C7—C15	1.442 (3)	C7′—C15′	1.448 (14)
C7—C1	1.483 (4)	C7′—C1′	1.483 (15)
C15—N2	1.146 (5)	C15′—N2′	1.148 (17)
C1—C6	1.402 (4)	C1′—C6′	1.377 (16)
C1—C2	1.402 (4)	C1′—C2′	1.410 (18)
C2—C3	1.382 (5)	C2′—C3′	1.40 (2)
C2—H2	0.9500	C2′—H2′	0.9500
C3—C4	1.393 (5)	C3′—C4′	1.41 (2)
C3—H3	0.9500	C3′—H3′	0.9500
C4—C5	1.390 (4)	C4′—C5′	1.376 (17)
C4—H4	0.9500	C4′—H4′	0.9500
C5—C6	1.384 (4)	C5′—C6′	1.369 (16)
C5—H5	0.9500	C5′—H5′	0.9500
C6—H6	0.9500	C6′—H6′	0.9500
Cl1′—C12′	1.735 (15)		
C13—C12—C11	121.7 (3)	C13′—C12′—C11′	122.6 (16)
C13—C12—Cl1	118.7 (2)	C13′—C12′—Cl1′	118.0 (14)
C11—C12—Cl1	119.6 (3)	C11′—C12′—Cl1′	119.1 (15)
C10—C11—C12	118.1 (4)	C10′—C11′—C12′	118 (2)
C10—C11—H11	120.9	C10′—C11′—H11′	120.8
C12—C11—H11	120.9	C12′—C11′—H11′	120.8
C11—C10—C9	122.1 (3)	C11′—C10′—C9′	121.2 (19)

C11—C10—H10	119.0	C11′—C10′—H10′	119.4
C9—C10—H10	119.0	C9′—C10′—H10′	119.4
C10—C9—C14	118.2 (3)	C14′—C9′—C10′	118.6 (14)
C10—C9—C8	117.6 (2)	C14′—C9′—C8′	122.3 (14)
C14—C9—C8	124.2 (2)	C10′—C9′—C8′	119.1 (15)
C13—C14—C9	120.7 (2)	C13′—C14′—C9′	122.5 (15)
C13—C14—H14	119.6	C13′—C14′—H14′	118.8
C9—C14—H14	119.6	C9′—C14′—H14′	118.8
C14—C13—C12	119.0 (2)	C14′—C13′—C12′	116.7 (15)
C14—C13—H13	120.5	C14′—C13′—H13′	121.6
C12—C13—H13	120.5	C12′—C13′—H13′	121.6
C7—C8—C9	129.4 (2)	C7′—C8′—C9′	130.8 (14)
C7—C8—H8	115.3	C7′—C8′—H8′	114.6
C9—C8—H8	115.3	C9′—C8′—H8′	114.6
C8—C7—C15	120.9 (2)	C8′—C7′—C15′	120.8 (13)
C8—C7—C1	124.3 (2)	C8′—C7′—C1′	124.7 (12)
C15—C7—C1	114.7 (2)	C15′—C7′—C1′	114.4 (13)
N2—C15—C7	177.6 (5)	N2′—C15′—C7′	173 (5)
C6—C1—C2	118.2 (3)	C6′—C1′—C2′	114.6 (15)
C6—C1—C7	120.6 (3)	C6′—C1′—C7′	123.4 (15)
C2—C1—C7	121.1 (3)	C2′—C1′—C7′	121.9 (16)
C3—C2—C1	120.7 (3)	C3′—C2′—C1′	119 (2)
C3—C2—H2	119.7	C3′—C2′—H2′	120.4
C1—C2—H2	119.7	C1′—C2′—H2′	120.4
C2—C3—C4	120.8 (4)	C2′—C3′—C4′	123 (2)
C2—C3—H3	119.6	C2′—C3′—H3′	118.6
C4—C3—H3	119.6	C4′—C3′—H3′	118.6
C5—C4—C3	118.9 (3)	C5′—C4′—C3′	115.1 (18)
C5—C4—H4	120.6	C5′—C4′—H4′	122.5
C3—C4—H4	120.6	C3′—C4′—H4′	122.5
C6—C5—C4	120.8 (3)	C6′—C5′—C4′	120.5 (17)
C6—C5—H5	119.6	C6′—C5′—H5′	119.8
C4—C5—H5	119.6	C4′—C5′—H5′	119.8
C5—C6—C1	120.6 (3)	C5′—C6′—C1′	125.6 (17)
C5—C6—H6	119.7	C5′—C6′—H6′	117.2
C1—C6—H6	119.7	C1′—C6′—H6′	117.2
C12′—Cl1′—Cl1′^{i}	122.6 (7)		

C13—C12—C11—C10	−4.3 (8)	Cl1′^{i}—Cl1′—C12′—C11′	−142.8 (8)
Cl1—C12—C11—C10	177.0 (4)	C13′—C12′—C11′—C10′	−0.02 (15)
C12—C11—C10—C9	1.2 (9)	Cl1′—C12′—C11′—C10′	174.0 (14)
C11—C10—C9—C14	2.3 (7)	C12′—C11′—C10′—C9′	0.02 (15)
C11—C10—C9—C8	−179.1 (5)	C11′—C10′—C9′—C14′	−0.1 (3)
C10—C9—C14—C13	−2.9 (4)	C11′—C10′—C9′—C8′	178.7 (14)
C8—C9—C14—C13	178.7 (3)	C10′—C9′—C14′—C13′	0.1 (5)
C9—C14—C13—C12	−0.1 (4)	C8′—C9′—C14′—C13′	−178.6 (15)
C11—C12—C13—C14	3.8 (6)	C9′—C14′—C13′—C12′	−0.1 (4)
Cl1—C12—C13—C14	−177.5 (2)	C11′—C12′—C13′—C14′	0.1 (3)

C10—C9—C8—C7	152.5 (3)	Cl1′—C12′—C13′—C14′	−174.0 (14)
C14—C9—C8—C7	−29.0 (5)	C14′—C9′—C8′—C7′	−31 (3)
C9—C8—C7—C15	−0.2 (4)	C10′—C9′—C8′—C7′	150.5 (17)
C9—C8—C7—C1	−176.9 (2)	C9′—C8′—C7′—C15′	−1 (3)
C8—C7—C1—C6	154.5 (3)	C9′—C8′—C7′—C1′	178.5 (17)
C15—C7—C1—C6	−22.4 (3)	C8′—C7′—C1′—C6′	155 (2)
C8—C7—C1—C2	−25.4 (4)	C15′—C7′—C1′—C6′	−25 (3)
C15—C7—C1—C2	157.7 (3)	C8′—C7′—C1′—C2′	−29 (3)
C6—C1—C2—C3	−0.5 (4)	C15′—C7′—C1′—C2′	151 (2)
C7—C1—C2—C3	179.5 (3)	C6′—C1′—C2′—C3′	8 (5)
C1—C2—C3—C4	0.5 (4)	C7′—C1′—C2′—C3′	−168 (4)
C2—C3—C4—C5	−0.7 (4)	C1′—C2′—C3′—C4′	−18 (8)
C3—C4—C5—C6	0.9 (4)	C2′—C3′—C4′—C5′	13 (7)
C4—C5—C6—C1	−0.9 (4)	C3′—C4′—C5′—C6′	1 (5)
C2—C1—C6—C5	0.6 (4)	C4′—C5′—C6′—C1′	−10 (4)
C7—C1—C6—C5	−179.3 (2)	C2′—C1′—C6′—C5′	5 (4)
Cl1′^{i}—Cl1′—C12′—C13′	31.4 (14)	C7′—C1′—C6′—C5′	−178 (2)

Symmetry code: (i) −*x*+1, *y*, −*z*+1/2.

Hydrogen-bond geometry (Å, º)

*Cg*1 and *Cg*2 are the centroids of rings C1–C6 and C9–C14 of the major disordered component. *Cg*1′ and *Cg*2′ are the centroids of rings C1′–C6′ and C9′–C14′ of the minor disordered component.

D—H···*A*	*D*—H	H···*A*	*D*···*A*	*D*—H···*A*
C5—H5···Cl1′^{i}	0.95	2.69	3.292 (5)	122
C8—H8···N2^{ii}	0.95	2.46	3.361 (6)	157
C8—H8···N2′^{ii}	0.95	2.53	3.44 (4)	160
C14—H14···N2′	0.95	2.54	3.22 (6)	129
C3—H3···*Cg*1^{iii}	0.95	2.99	3.860 (4)	153
C3—H3···*Cg*2′^{iii}	0.95	2.95	3.784 (9)	148
C11—H11···*Cg*2^{iv}	0.95	2.96	3.418 (7)	111
C11—H11···*Cg*1′^{iv}	0.95	2.97	3.486 (15)	115
C14—H14···*Cg*1^{v}	0.95	2.81	3.503 (3)	130
C14—H14···*Cg*2′^{v}	0.95	2.84	3.585 (8)	136
C3′—H3′···*Cg*2^{iv}	0.95	2.59	3.32 (6)	134
C3′—H3′···*Cg*1′^{iv}	0.95	2.62	3.39 (6)	139
C6′—H6′···*Cg*1^{v}	0.95	2.85	3.52 (2)	129
C6′—H6′···*Cg*2′^{v}	0.95	2.93	3.64 (2)	132

Symmetry codes: (i) −*x*+1, *y*, −*z*+1/2; (ii) *x*−1/2, −*y*+1/2, −*z*+1; (iii) −*x*+1/2, *y*−1/2, *z*; (iv) −*x*+1/2, *y*+1/2, *z*; (v) −*x*+1, −*y*, −*z*+1.